Synthesis and properties of phosphonic acid-grafted hybrid inorganic–organic polymer membranes

Siwen Li,[a] Zhen Zhou,[a] Harry Abernathy,[a] Meilin Liu,*[a] Wen Li,[b] Junzo Ukai,[b] Kohei Hase[c] and Masatsugu Nakanishi[c]

Received 1st September 2005, Accepted 7th December 2005
First published as an Advance Article on the web 19th December 2005
DOI: 10.1039/b512389e

A class of phosphonic acid-grafted hybrid inorganic–organic polymer membranes was synthesized using a sol–gel process. Their thermal stability, water uptake, and proton conductivity were investigated. TGA–DSC analysis indicated that these membranes are thermally stable up to at least 220 °C in dry air. The proton conductivities of the new membranes increase with $–PO_3H_2$ group content and relative humidity, reaching 6.2×10^{-2} S cm^{-1} at 100 °C with ~100% relative humidity, comparable to those of Nafion® under similar conditions. These new membranes have high proton conductivity at low relative humidity and thus have great potential to be used as electrolytes for high-temperature, low-humidity PEM fuel cells and other electrochemical applications. The proton conductivity of the membranes in the anhydrous state was enhanced by substitution of $–CH_2–PO_3H_2$ groups with $–CF_2–PO_3H_2$ groups owing to the large electron-withdrawing effect of C–F bonds. However, it was found that the concentration of $–PO_3H_2$ groups and the molecular structures of the new membranes are the key factors for the proton transport process in a humidified environment.

1. Introduction

Proton exchange membranes (PEMs) are a critical component in fuel cells, hydrogen separation/purification, reforming/partial oxidation of hydrocarbon fuels, contaminant removal, gas sensing, and other processes relevant to energy storage and conversion. While various electrolyte membranes have been studied for many years, the existing membranes are still inadequate in performance for the intended applications. The widely used perfluorosulfonic polymers (mainly Nafion®) have relatively low proton conductivity over 100 °C, large amount of gas crossover, significant dimensional changes with water content, high cost, and the decomposition of $–SO_3H$ groups under fuel cell working conditions.[1–7] These limitations have stimulated intense interest in the development of new proton conducting membranes, including polymer proton electrolytes with nanometer-sized hygroscopic metal oxides,[8,9] sulfonated aromatic polymer membranes, polymer–H_3PO_4 membranes,[10–12] and hybrid inorganic–organic proton conducting membranes doped with proton-conductive components, including H_3PO_4, heteropolyacids, and grafted $–SO_3H$ groups.[12–16]

Hybrid inorganic–organic polymers have been extensively studied as PEMs in which inorganic networks are cross-linked through organic chains on a molecular scale. Proton-conductive compounds $Zr(HPO_4)_2 \cdot H_2O$, silicotungstic acid, and 12-phosphotungstic acid have been introduced into hybrid polymers.[3,13–15] In these membranes, large amounts of inorganic compounds are necessary for high proton conductivity, thus limiting the mechanical properties of the membranes. Sulfonic acid group-grafted hybrid inorganic–organic copolymer membranes displayed high proton conductivities under conditions of high relative humidity below 100 °C, similar to Nafion® membranes.[1,16] However, they have very limited thermal stability because of the strong acidity and the oxidizing effect of sulfonic acid groups.[16]

Here we report a series of new proton conducting membranes based on hybrid inorganic–organic polymers with grafted $–PO_3H_2$ groups or $–CF_2–PO_3H_2$ groups. $–PO_3H_2$ groups are stable in reducing environments and have higher water holding ability than $–SO_3H$ groups.[12] The new membranes were synthesized through a simple sol–gel process. Membranes of thickness less than 0.1 mm can be readily cast. Compared to Nafion® membranes, the new hybrid inorganic–organic membranes have comparable proton conductivities but with much less dependence on humidification.

2. Experimental

2.1 Synthesis of precursors

Phosphonic acid groups were grafted onto the hybrid inorganic–organic copolymer networks through a short organic chain *via* Si–C bonds. The precursors used in this study are diethyl-4-(diethoxy(methyl)silyl)-1,1-difluorobutyl-phosphonate (FP, see Scheme 1) and diethoxyphosphoryl-ethyltriethoxysilane (CP, Gelest, 95%, see Scheme 2). FP was synthesized according to Scheme 1, where compound (**2**) was synthesized as described elsewhere.[17] In a typical experiment,

[a]*Center for Innovative Fuel Cell and Battery Technologies, School of Materials Science and Engineering, Georgia Institute of Technology, Atlanta, GA, 30332-0245, USA. E-mail: meilin.liu@mse.gatech.edu; Fax: +1-404-894-9140; Tel: +1-404-894-6114*
[b]*Materials Engineering Department, Toyota Technical Center, USA, Inc., Ann Arbor, MI 48105, USA*
[c]*Material Engineering Division II, Vehicle Engineering Group, Toyota Motor Corporation, Toyota, Aichi 471-8572, Japan*

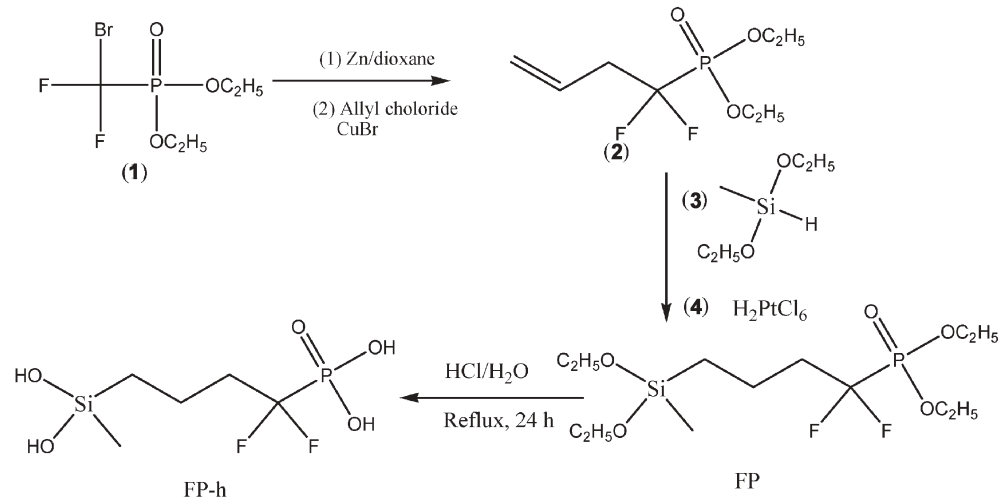

Scheme 1 Synthesis process of FP and its hydrolyzed form FP-h.

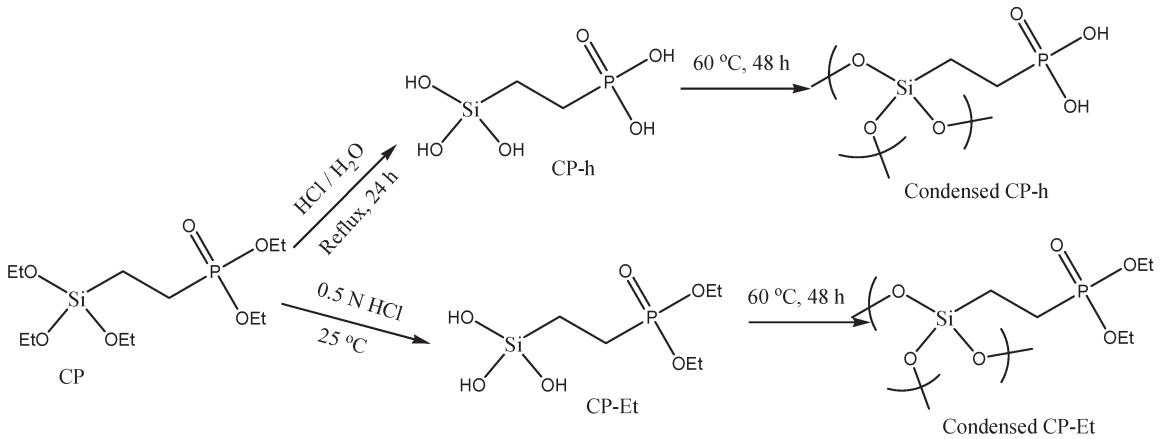

Scheme 2 Hydrolysis of CP to CP-h and CP-Et, and corresponding condensed forms.

4.8 g (23.4 mmol) of compound (**2**) was mixed with 7.5 g (56 mmol) diethoxymethylsilane (**3**) and several drops of hydrogen hexachloroplatinate (**4**) solution (5% in isopropanol). After stirring at 60 °C overnight, the solution was evaporated under reduced pressure to remove the reactants and product FP was obtained (6.0 g, 16.6 mmol, yield 71%). ^{1}H NMR ($CDCl_3$): δ (ppm) 0.12 (3H, s), 0.65 (2H, m), 1.21 (6H, t, J_{H-H} = 6.98), 1.35 (6H, 6, J_{H-H} = 7.06), 1.65 (2H, m), 2.15 (2H, m), 3.75 (4H, q, J_{H-H} = 6.98), 4.26 (4H, q, J_{H-H} = 7.06).

2.2 Hydrolysis of diethoxyphosphoryl groups

The precursors FP and CP were hydrolyzed before use to change diethoxyphosphoryl groups to phosphonic acid groups in condensed hydrochloric acid as shown in Schemes 1 and 2.[18] The process can be described with CP as an example: 3.28 g CP ($\sim$10 mmol) was dissolved in 50 ml of condensed hydrochloric acid aqueous solution by stirring in a three-necked flask with a condenser and an argon (Ar) gas line. The flask (under the protection of Ar) was immersed in an oil bath and kept at 90 °C for about 24 hours. After cooling down to 50 °C, the hydrochloric acid aqueous solution was evaporated under reduced pressure, and transparent viscous solid dihydroxyphosphorylethyltrihydroxysilane (CP-h) was obtained with a yield of 100%. The hydrolyzed form of FP, labeled as FP-h, is insoluble in condensed hydrochloric acid aqueous solution and water, but soluble in ethanol and methanol.

When CP was hydrolyzed in ethanol catalyzed with 0.5 N HCl aqueous solution, only $-Si(OC_2H_5)_3$ will be changed to $-Si(OH)_3$, while the $-PO(OC_2H_5)_2$ groups will remain stable in this process (see Scheme 2). This partially hydrolyzed form was labeled as CP-Et. Condensed CP-Et and condensed CP-h were obtained by heating in air at 60 °C for several days.

2.3 Preparation of membranes

CP-h or FP-h were dissolved in ethanol together with bis[(3-methyldimethyoxysilyl)propyl]polypropylene oxide (M, Gelest, 96%; MW 600–900, see Scheme 3), 1,4-bis(trimethoxysilylethyl)benzene (Be, Gelest, 98%, see Scheme 3), bis(triethoxysilyl)octane (Oc, Gelest, 98%, see Scheme 3), tetraethoxysilane (T), and/or (3-glycidoxypropyl)triethoxysilane (G, Scheme 3) (Alfa, 96%). After stirring for 20 minutes, 0.5 N HCl aqueous solution was added dropwise to the precursor solution, and further stirred for 12 to 48 hours. The

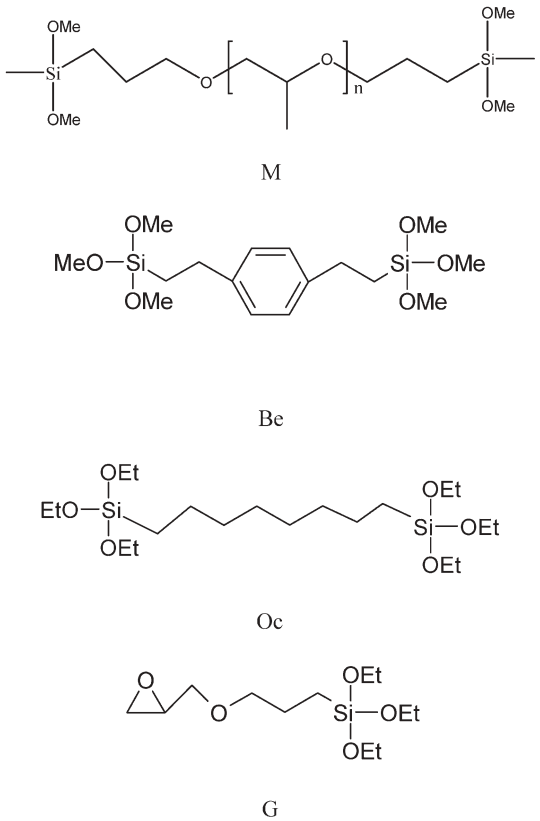

Scheme 3 Molecule structures of precursors as network formers.

sols were cast on petri dishes. The amount of water added is 4 times of the total amount of Si in mol. The membranes were dried at 60 °C for 3 days, at 80 °C for 3 hours, and then at 100 °C for 1 hour to evaporate the organic solvents and water. The samples were labeled by their mole composition as *x*M-*y*Be (or Oc)-*z*CP (or FP), where *x*, *y*, and *z* represent the number of moles of Si from M, Be (or Oc), and CP-h (or FP-h), respectively. Typical values for *x* are 1–2, *y* 2–4, and *z* 3–6. The samples with G were labeled as *x*G-*y*T-*z*CP, where *x*, *y*, and *z* represent the number of moles of Si from G, T, and CP-h, respectively. The typical values of *x*, *y*, and *z* were 0–2, 0–2, and 2, respectively.

2.4 Characterization of membranes

X-Ray diffraction patterns of the membranes were obtained using a Philips PW 1800 diffractometer with Cu K_α radiation. Fourier transform infrared (FTIR) spectroscopy measurements were performed on thin pellets composed of 5% sample and 95% KBr using a Bruker Equinox 55 spectrometer. Each spectrum presented is the sum of 64 scans at 4 cm^{-1} resolution. Thermogravimetric analysis (TGA) and differential scanning calorimetry (DSC) were performed in a Pt crucible with about 20 mg of samples using a Rheometric Scientific STA 1500 in dry air from room temperature to 500 °C. ^1H NMR spectra was recorded with a Varian Mercury Vx 300 spectrometer operating at 300 MHz. Solid state ^{31}P MAS-NMR spectra were acquired using a Bruker DSX 400 spectrometer operating at 161.86 MHz. The ^{31}P signal from $NH_4H_2PO_4$ at 298 K was referenced to $\delta = 0$ ppm. Small pieces of membranes were used to measure the proton conductivity using a SI 1255 frequency response analyzer and SI 1286 potentiostat/galvanostat in the frequency range of 0.01 Hz to 5 MHz. Two gold-coated silver pellets were used as the electrodes. The samples were kept at each temperature for 4–8 hours until the electrical responses of the samples became stable. Relative humidity (RH) of 100% was maintained by excess water whereas RHs of 20% and 75% were supplied by a saturated aqueous solution of $MgCl_2$ and KCl, respectively, in a closed chamber.[19]

3. Results and discussion

3.1 Formation of hybrid inorganic–organic polymers

Shown in Fig. 1 are the FTIR spectra of condensed CP-h, condensed CP-Et, a membrane with a composition of 2M-4Be-4CP, and a membrane with a composition of 2M-2Be-6CP. The FTIR spectrum of condensed CP-Et has a strong peak at 2980 cm^{-1}, corresponding to the $-CH_3$ group in $-PO(OC_2H_5)_2$. This peak disappeared from the spectrum of condensed CP-h, but a broad peak corresponding to –P–O–H groups appeared at 2320 cm^{-1}, indicating that the $-PO(OC_2H_5)_2$ group was hydrolyzed and changed to $-PO_3H_2$.[20] The strong peak of Si–O–Si asymmetric stretching vibration was observed at 1030 cm^{-1} in the spectra of condensed CP-h and CP-Et, and at 1100 cm^{-1} in those of the membranes with compositions of 2M-4Be-4CP and 2M-2Be-6CP.[21] This indicates that the inorganic backbone –Si–O–Si–O– was formed in the drying process. X-Ray analysis of the membranes indicated that the as-prepared membranes were nearly amorphous. There was only one weak broad peak near $2\theta = 22°$ in the XRD spectra (see Fig. 2), which may be assigned to the typical coherent diffraction domains of Si–O based backbones of the hybrid inorganic–organic polymers.[22,23] The XRD results further confirmed the formation of Si–O–Si based hybrid inorganic–organic polymer networks in the new membranes.

All as-prepared membranes were transparent, self-standing, and flexible (see Fig. 3). Self-standing membranes with a thickness of less than 100 μm can be cast readily to large sizes depending on the molds. It should be mentioned that the sols

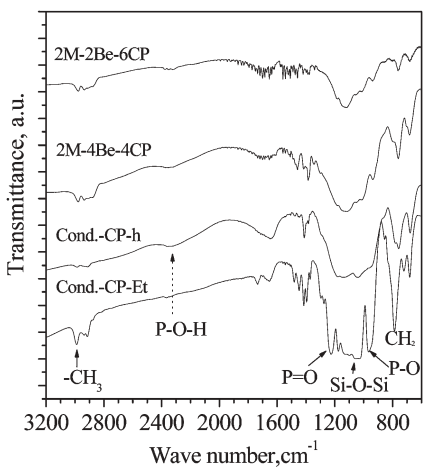

Fig. 1 FTIR spectra of condensed CP-h, condensed CP-Et, and the membranes with compositions of 2M-4Be-4CP and 2M-2Be-6CP.

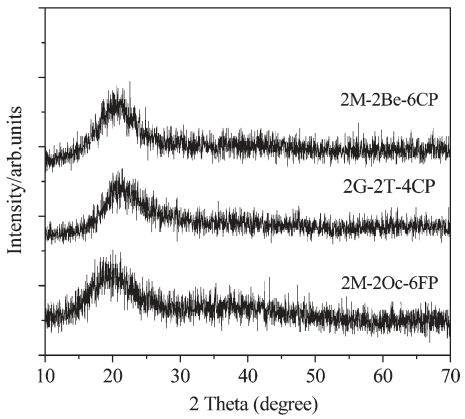

Fig. 2 XRD patterns of the hybrid inorganic–organic polymers with grafted $–PO_3H_2$ groups.

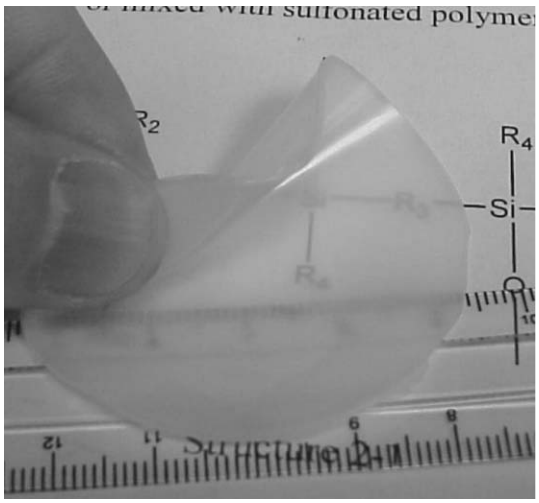

Fig. 3 Appearance of the membrane with a composition of 2M-2T-6CP.

with $–CF_2–PO_3H_2$ groups must be stirred at room temperature for at least 48 hours to form thick sols. If the sols are too thin, the obtained membranes display severe phase separation: a brittle upper layer (mainly composed of the condensed FP-h) and a soft lower layer (mainly composed of the hybrid inorganic–organic copolymers introduced by the precursor M). The shrinkage of the membranes in the drying process decreases with increasing G or M content. The volumetric shrinkage rate of 1Be-1CP is about 50%, but there was no observable shrinkage for the membranes with composition of 2M-2Oc (or Be)-6CP and 1G-1CP. The membranes with G become very soft above 80 °C in the atmosphere with relative humidity close to 100% when the content of precursor G is high (G/CP > 1 in mol). The membranes with compositions of *x*M-*y*Oc (or Be)-*z*CP (or FP) are more flexible when saturated with water than in anhydrous states, but retain adequate mechanical strength at temperatures up to 120 °C with ~100% relative humidity.

3.2 Status of $–PO_3H_2$ groups in the membranes

^{31}P NMR spectra of the membranes with compositions of 2M-4Be-4CP and 2M-2Oc-6FP were acquired to further check

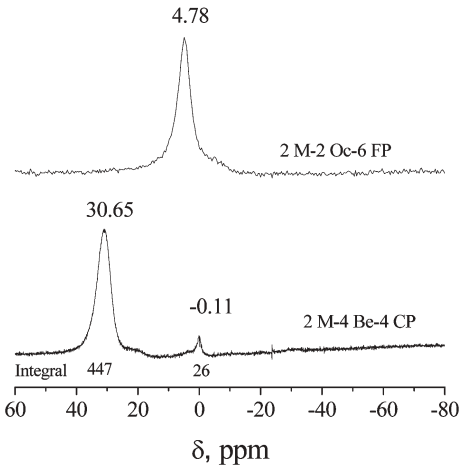

Fig. 4 ^{31}P NMR spectra of the membranes with compositions of 2M-2Oc-6FP and 2M-2Be-4CP.

the status of the phosphoric acid groups in the membranes (see Fig. 4). In the spectrum of the membrane 2M-4Be-4CP, two ^{31}P resonance peaks were observed at $\delta = -0.1$ ppm and +30.65 ppm, respectively. The extremely strong peak at $\delta =$ 30.65 ppm is attributed to the $–PO_3H_2$ groups grafted on aliphatic chains *via* C–P bonds.[24–26] To assign the weak peak at $\delta = -0.11$ ppm, the liquid ^{31}P NMR spectrum of the starting reagent CP (95%) was checked, revealing a strong peak at 33.9 ppm and a weak peak at 7.95 ppm. The integral of the weak one is 1.2% of total. This weak peak is from an unknown impurity of the starting agent CP.[24] Although the integral of the weak peak at −0.11 ppm in the spectrum of the sample 2M-4Be-4CP is about 4.3% of the total, further investigation may be necessary to confirm the assignment of the weak peak. Only one strong peak at 4.78 ppm was observed in the ^{31}P NMR spectrum of the membrane with grafted $–CF_2–PO_3H_2$ groups. Compared with that of $–CH_2–PO_3H_2$ groups, the ^{31}P NMR peak of $–CF_2–PO_3H_2$ moved much to the negative side, confirming that the $–CF_2–$ group has a strong electron-withdrawing effect on the $–PO_3H_2$ groups. It is noted that all the $–PO_3H_2$ groups in the membranes did not react with SiO networks in the new hybrid inorganic–organic membranes to form Si–O–P bonds. These acid groups will act as proton donors and acceptors and make a contribution to proton conduction.

3.3 Thermal and chemical stability of the membranes

Shown in Fig. 5 are the TGA curves of several samples together with the DSC curve of a sample with composition of 1G-1CP in dry air from room temperature to 500 °C. There are mainly two mass-loss steps in the TGA curves. The small weight loss below the decomposition temperatures corresponds to the evaporation of the small organic molecules and water including that produced by the condensation of $–PO_3H_2$ groups in the membranes. The decomposition of the organic part of the copolymers starts from 220 °C, 240 °C, 250 °C and 280 °C for the membranes with composition of 2M-2Oc-6CP, 2M-4Be-4CP, 2M-2Oc-6FP, and 1G-1CP, respectively. Correspondingly exothermic peaks near the

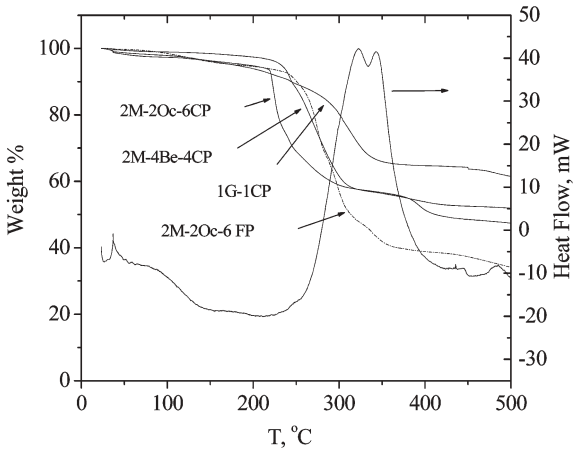

Fig. 5 TGA–DSC curves of the membranes with $-PO_3H_2$ groups as measured in dry air with a heating rate of 5 °C min^{-1}. The DSC curve is for the membrane with a composition of 1G-1CP.

decomposition temperature appear in the DSC curves. The hybrid inorganic–organic membranes are therefore stable up to 220 °C in dry air.

The chemical stability was examined by immersing a piece of sample (0.5 cm × 1 cm) in a standard Fenton reagent (3% H_2O_2 aqueous solution with 2 ppm $FeSO_4$) at 80 °C.[27] It was found that the samples derived from precursor CP, FP and network formers M, Be and Oc were stable (no dissolution, no cracking, and no visible changes in mechanical flexibility and strength) after immersion in the solution at 80 °C for 24 hours. These results suggest that the new membranes have good chemical stability for fuel cell applications.

3.4 Proton conductivity in anhydrous state

Shown in Fig. 6 are the proton conductivities measured in dry Ar of the membranes after being dried at 80 °C for 6 hours and 100 °C for 2 hours. The proton conductivity of all the membranes increased with temperature, reaching 1.2 × 10^{-4} S cm^{-1} at 120 °C for the membrane with a composition

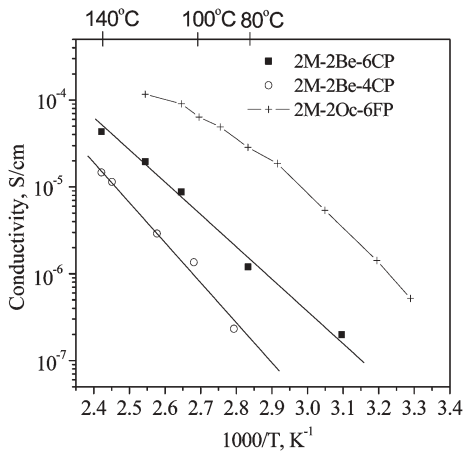

Fig. 6 Proton conductivities of membranes with grafted $-PO_3H_2$ groups as measured in dry argon.

of 2M-2Oc-6FP. Comparing the conductivity data of the membranes 2M-2Be-4CP and 2M-2Be-6CP, the proton conductivity increased with $-PO_3H_2$ content, suggesting that the dissociation among the $-PO_3H_2$ groups grafted on the hybrid inorganic–organic copolymer network contributed to proton conduction in the membranes through the Grotthuss mechanism.[26,28] The sample with grafted $-CF_2-PO_3H_2$ groups had a higher proton conductivity than that with grafted $-CH_2-PO_3H_2$ groups when they had the same $-PO_3H_2$ content. This can be attributed to the fact that $-CF_2-PO_3H_2$ groups have higher acidity because of the large electron-withdrawing effect of $-CF_2-$ groups. The dissociation among $-CF_2-PO_3H_2$ groups can produce more mobile protons for transport than $-CH_2-PO_3H_2$ groups.[29] The higher proton conductivity of the membrane with grafted $-CF_2-PO_3H_2$ groups may have some relation to its structural characteristics. However, it has to be pointed out that the structural characteristics of the membrane with grafted $-CF_2-PO_3H_2$ groups may contribute to the observed high proton conductivity as well. The chain that connects $-CF_2-PO_3H_2$ with Si is longer than that connecting $-CH_2-PO_3H_2$ with Si (see Schemes 1 and 2). Meanwhile, the polymers derived from FP were more flexible than those derived from CP because FP contains diethoxy(methyl)silyl groups, and the backbone of the polymers derived from FP is more linear. The grafted $-CF_2-PO_3H_2$ groups have higher local mobility, and the protons can be transported faster *via* structure diffusion (Grotthuss mechanism).[28]

3.5 Water uptake

The water uptake rate in relative humidity 100% was calculated by the weight change between the dried (in dry Ar at 70 °C for about 12 hours) and water-saturated (in closed water chamber for 24 hours at room temperature) samples. As summarized in Table 1, one mole of $-PO_3H_2$ groups in the hybrid inorganic–organic polymer membranes absorb 2.6–5.2 moles of water, depending on the composition of the membrane. Compared with polymers such as poly(vinyl acrylate phosphoric acid) and phosphonic acid functionalized poly(aryloxyphosphazene), in which one mole of acid groups can usually absorb at least 12 moles of water,[12,30,31] the new hybrid inorganic–organic membranes with $-PO_3H_2$ groups absorbed much less water. It was reported that the water uptake of polymer materials with grafted acid groups is controlled by the molecular structures of the materials.[12] For

Table 1 Proton conductivity and water uptake of the membranes

	Conductivity/S cm^{-1}		Water uptake		
Composition	25 °C	100 °C	Weight%	[H_2O/–PO_3H_2]	E_a/eV
2M-4Be-4CP	—	5.8×10^{-3}	10.8	2.6	0.70
2M-2Be-4CP	1.0×10^{-3}	8.5×10^{-3}	15.0	3.1	0.26
2M-2Be-6CP	1.3×10^{-3}	2.2×10^{-2}	26.5	4.4	0.27
2M-2Oc-6CP	1.5×10^{-3}	6.2×10^{-2}	23.6	5.1	0.32
2M-2Oc-6FP	—	1.1×10^{-2}	13.6	5.4	0.05/ 1.5[a]
4Oc-6FP	2.2×10^{-3}	5.0×10^{-2}	25.2	5.2	0.30

[a] E_a value below 70 °C.

example, in S-PPBP (sulfonated poly(4-phenoxybenzoyl-1,4-phenylene)) and S-PEEK (sulfonated poly(oxy-1,4-phenyleneoxy-1,4-phenylenecarbonyl-1,4-phenylene)), one mole of $–SO_3H$ can absorb 9 and 3 moles of water, respectively, in relative humidity 100% at room temperature owing to the flexible side chains of S-PPBP.[3,12] The lower water uptake of the new hybrid inorganic–organic copolymer membranes may be attributed to the tight inorganic –Si–O–Si–O– networks.

3.6 Humidity dependence of proton conductivity

Shown in Fig. 7 is the humidity dependence of the proton conductivity of the membrane with a composition of 2M-2Oc-6CP at 80 °C and 100 °C. The proton conductivity at 80 °C increases from 10^{-6} S cm^{-1} in dry argon to 2.3×10^{-3} S cm^{-1} at ~20% RH and 1.76×10^{-2} S cm^{-1} at ~100% RH. The dramatic increase in the proton conductivity of these membranes in wet atmosphere can be attributed to the fast transport of H_3O^+ in a vehicle mechanism.[28,29] Comparing the proton conductivity dependence on RH of the new hybrid inorganic–organic membranes with that of most sulfonated-aromatic polymers,[12] one can find that the new membranes with grafted $–PO_3H_2$ groups display much higher proton conductivity in low RH. For example, the proton conductivity of sulfonated poly(oxy-1,4-phenyleneoxy-1,4-phenylenecarbonyl-1,4-phenylene) (S-PEEK, 65% sulfonation) is less than 10^{-6} S/ cm^{-1} at RH <50%.[12] The new membrane with a composition of 2M-2Oc-6CP had a proton conductivity similar to Nafion® 117 at 80 °C and 100 °C at both low RH and high RH (see Fig. 7).

The proton conductivities of all obtained membranes were measured at ~100% RH from room temperature to 100 °C. The membranes with precursor G had a proton conductivity of 10^{-3} S cm^{-1} below 80 °C. Shown in Fig. 8 is the temperature dependence of proton conductivities of the precursor M-based membranes. The proton conductivity increased with $–PO_3H_2$ content, and reached 10^{-2} S cm^{-1} at 100 °C when the molar ratio of $–PO_3H_2$/Si was larger than 0.5 in the membranes. It was 6.2×10^{-2} S cm^{-1} for the sample with a composition of

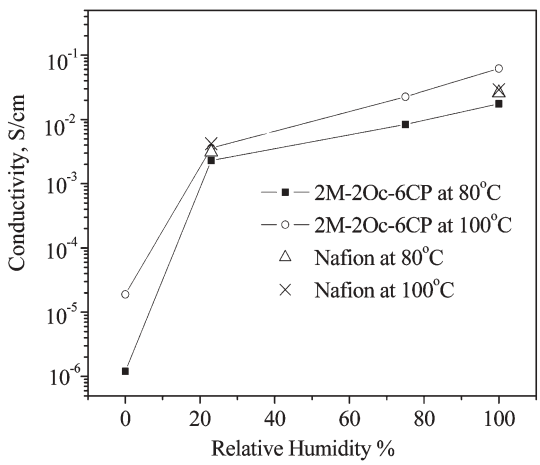

Fig. 7 Humidity dependence of the proton conductivity of a membrane with composition of 2M-2Oc-6CP at 80 °C and 100 °C, compared with those of Nafion 117.

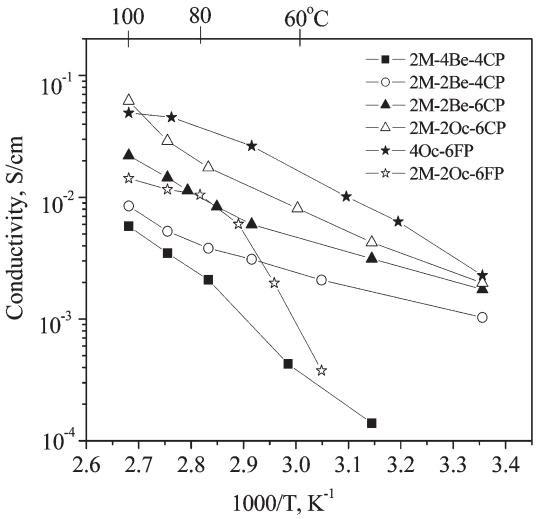

Fig. 8 Proton conductivity measured at 100% relative humidity of membranes with compositions of xM-yBe-zCP ($x = 2$, $y = 2$ and 4, $z = 4$ and 6), 2M-2Oc-6CP, 2M-2Oc-6FP, and 4Oc-6FP.

2M-2Oc-6CP at 100 °C. The proton conductivity of the new hybrid inorganic–organic membranes is comparable with that of Nafion® and sulfonated aromatic polymer membranes,[12,30,32] and much higher than other polymer membranes with $–PO_3H_2$ groups, for example, phosphoxyethyl-trifloroethylacrylate (PHM-TFEA) copolymer membranes (about 5×10^{-3} S cm^{-1} at 100 °C and 100% RH).[12,30] The high proton conductivity of the new hybrid inorganic–organic copolymer membranes was achieved with a smaller amount of water compared with other polymer membranes. The water uptake in polymer membranes includes two parts: one is for solvation of the protons and acid groups, the other for polymer swelling.[12] The water uptake of the hybrid inorganic–organic copolymer membrane grafted $–PO_3H_2$ groups is enough for the solvation of acid groups and for fast transport of H_3O^+ ions. This may be related to the specific hybrid inorganic–organic network in the new membranes based on a tight –Si–O–Si–O– inorganic backbone and highly flexible organic chains formed by PPO because these networks as good proton acceptors may assist proton transport.[33]

It is noted that the membranes derived from precursor Oc has higher proton conductivity than those derived from precursor Be when they have the same content of $–PO_3H_2$ groups. The main reason may be that $–PO_3H_2$ groups in the membrane with Oc can absorb a little more H_2O than those in the membrane with Be. Another reason is that the aliphatic chains introduced by Oc are more flexible than the aromatic ring containing chains introduced by Be. The membrane with flexible Oc chains may have larger domains in which water can form pathways for proton transport.[12,34] However, it is still difficult to explain the behavior of the membranes derived from FP; the membrane with composition of 2M-2Oc-6FP has lower proton conductivity than 2M-2Oc-6CP and 2M-2Be-6CP although it has a more flexible network owing to its linear structure derived from the methyldihydroxysilyl groups in precursor FP-h (see Scheme 1). In contrast, the sample with higher content of cross-linker, 4Oc-6FP, has much higher

proton conductivity than 2M-2Oc-6FP (see Fig. 8). These results indicate that the higher acidity of $–CF_2–PO_3H_2$ groups may have little effect on the proton conductivity of the membranes in a high RH environment, but the morphologies and the molecular structures of the membranes are more important to the proton transport process.

Shown in Fig. 8 are the proton conductivities of all samples measured from room temperature to 100 °C. The Log $\sigma \sim 1/T$ curves of the samples, especially those derived from precursor CP-h, are nearly linear, indicating that the proton conductivity of these samples exhibits Arrhenius-type behavior. The activation energy was estimated from the slopes of the Arrhenius plots (Fig. 8). The average activation energy for the temperature range studied tends to decrease with increasing the content of the $–PO_3H_2$ group (see Table 1). The estimated average activation energy is 0.71 eV (68.5 KJ mol^{-1}) for the membrane 2M-4Be-4CP ($–PO_3H_2$/Si = 4/10 in mol) and about 0.3 e V (28.9 KJ mol^{-1}) for the other four membranes with higher contents of $–PO_3H_2$ groups. The latter value is comparable to that of Nafion® membranes, indicating that the new membranes may have a similar conduction mechanism involving the hydronium ions.[35] There is an obvious change of slope coefficient in the Log $\sigma \sim 1/T$ curve of the sample with composition 2M-2Oc-6FP, indicating an activation energy change near 70 °C. Comparing the Log $\sigma \sim 1/T$ curve of this sample in humidified environment with that in the anhydrous state, one can find that this activation energy change may be related with the changes in morphologies of this membrane with temperature under fully humidified conditions.

4. Conclusion

The new membranes with $–PO_3H_2$ groups grafted on the hybrid inorganic–organic networks formed among the alkoxysilanes M, Be, Oc, T, and G have good stability and high proton conductivity (>10^{-2} S cm^{-1} above 50 °C) under humidified conditions. Compared with the organic polymer membranes containing acid groups, the hybrid inorganic–organic copolymer membranes can achieve high proton conductivity with much less water and thus have much less dependence on humidity. They have great potential for application in PEM fuel cells and other electrochemical devices, especially for high temperature and low relative humidity. The physical state of water and the proton transport mechanism in these hybrid inorganic–organic membranes are yet to be determined, which would be essential to intelligent design of new membranes with high proton conductivity and adequate stability for practical applications.

List of Abbreviations

Oc: bis(triethoxysilyl)octane; Be: bis(trimethoxysilylethyl)-benzene; CP: diethoxyphosphorylethyltriethoxysilane; CP-Et: diethoxyphosphorylethyltrihydroxysilane; FP: diethyl-4-(diethoxy(methyl)silyl)-1,1-difluorobutylphosphonate; G: (3-glycidoxypropyl)triethoxysilane; FP-h: 4-(dihydroxy-(methyl)silyl)-1,1-difluorobutylphosphonate; M: bis[(3-methyl-dimethyoxysilyl)propyl]polypropylene oxide; CP-h: dihydroxyphosphorylethyltrihydroxysilane; T: tetraethoxysilane.

References

1 L. Depre, M. Ingram, C. Poinsignon and M. Popall, *Electrochim. Acta*, 2000, **45**, 1377–83.
2 K. D. Kreuer, *J. Memb. Sci.*, 2001, **185**, 29–39.
3 J. M. Bae, I. Honma, M. Murata, T. Yamamoto, M. Rikukawa and N. Ogata, *Solid State Ionics*, 2002, **147**, 189–94.
4 N. Chen and L. Hong, *Solid State Ioncs*, 2002, **146**, 377–85.
5 S. Surampudi, S. R. Narayanan, E. Vamos, H. Frank, G. Halpert, A. LaConti, J. Kosek, G. K. Surya Prakash and G. A. Olah, *J. Power Source*, 1994, **47**, 377–85.
6 A. J. Appleby and F. R. Foulkes, ed., *Fuel Cell Handbook*, Malabar, FL: Krieger, 1993.
7 K. Tsuruhara, M. Rikukawa, K. Sanui, N. Ogata, Y. Nagasaki and M. Kato, *Electrochim. Acta*, 2000, **45**, 1391–4.
8 M. Watanabe, H. Uchida and M. Emori, *J. Phys. Chem. B*, 1998, **102**, 3129–37.
9 H. Wang, B. A. Holmberg, L. Huang, Z. Wang, A. Mitra, J. M. Norbeck and Y. Yan, *J. Mater. Chem.*, 2002, **12**, 834–7.
10 J. S. Wainright, J.-T. Wang, D. Weng, R. F. Savinell and M. Lit, *J Electrochem Soc.*, 1995, **142**, L121.
11 A. Schechter and R. Savinell, *Solid State Ionics*, 2002, **147**, 181–7.
12 M. Rikukawa and K. Sanui, *Prog. Polym. Sci.*, 2000, **25**, 1463–502.
13 A. Matsuda, T. Kanzaki, Y. Yoshinori, M. Tatsuminago and T. Minami, *Solid State Ionics*, 2001, **139**, 113–9.
14 K. Hirata, A. Matsuda, T. Hirata, M. Tatsumisago and T. Minami, *J. Sol-gel Sci. Tech.*, 2000, **17**, 61–9.
15 A. Matsuda, T. Kanzaki, M. Tatsuminago and T. Minami, *Solid State Ionics*, 2001, **145**, 161–6.
16 M. Popall and X. M. Du, *Electrochim. Acta*, 1995, **40**, 2305–8.
17 W. Qiu and D. J. Burton, *Tetrahedron Lett.*, 1996, **37**, 2745–8.
18 D. J. Burton and L. G. Sprague, *J. Org. Chem.*, 1989, **54**, 613–7.
19 Th. Dippel, K. D. Kreuer, J. C. Lassegues and D. Rodriguez, *Solid State Ionics*, 1993, **61**, 41–6.
20 N. B. Colthup, L. H. Daly and S. E. Wiberley, *Introduction to Infrared and Raman Spectroscopy*, Academic Press, New York, 1964, p.403.
21 N. B. Colthup, L. H. Daly and S. E. Wiberley, *Introduction to Infrared and Raman Spectroscopy*, Academic Press, New York, 1964, p.324.
22 Y. Park and M. Nagai, *Solid State Ionics*, 2001, **145**, 149–60.
23 L. D. Carlos, V. de Zea Bermudez, R. A. Ferrerira, L. Marques and M. Assuncao, *Chem. Mater.*, 1999, **11**, 581–8.
24 P. Kohli and G. J. Blanchard, *Langmuir*, 2000, **16**, 695.
25 A. Aliev, D. Ou, B. Ormsby and A. C. Sullivan, *J. Mater. Chem.*, 2000, **10**, 275–81.
26 S. Li and M. Liu, *Electrochim. Acta*, 2003, **48**, 4271–5.
27 K. Miyatake, N. Asano and M. Watanabe, *J. Polym. Sci.: A*, 2003, **41**, 3901—.
28 K. D. Kreuer, *Chem. Mater.*, 1996, **8**, 610–41.
29 D. R. Lide, *CRC Handbook of Chemistry and Physics*, CRC Press, Boca Raton, Fla.0, 1998, p15–26.
30 K. Kaneko, Y. Takeoka, M. Aizawa and M. Rikukawa, *Synth. Met.*, 2003, **135–136**, 73–4.
31 H. R. Allcock, M. A. Hofmann, C. M. Ambler, S. N. Lvov, X. Y. Zhou, E. Chalkova and J. Weston, *J. Memb. Sci.*, 2002, **201**, 47–54.
32 K. Miyatake, H. Iyotani, K. Yamamoto and E. Tsuchida, *Macromole.*, 1996, **29**, 6969–71.
33 J. Qiao, N. Yoshimoto and M. Morita, *J. Power Sources*, 2002, **105**, 45–51.
34 M. A. Hickner and B. S. Pivovar, *Fuel Cells*, 2005, **5**, 213–29.
35 P. C. Rieke and N. E. Vanderborgh, *J. Memb. Sci.*, 1987, **32**, 313–28.

